In situ observation of correlations between domain switching and crack propagation in BaTiO$_3$ single crystals under coupling of mechanical and electric loads

Bing Jiang,[a,*] Yang Bai,[b,*] Meicheng Li[a] and Trevor Mwenya[a]

[a]State Key Laboratory of Alternate Electrical Power System with Renewable Energy Sources, School of Renewable Energy,
North China Electric Power University, Beijing 102206, China
[b]Corrosion and Protection Center, Key Laboratory for Environmental Fracture (Ministry of Education),
University of Science and Technology Beijing, Beijing 100083, China

Domain switching and crack propagation in BaTiO$_3$ single crystals under external mechanical and electric load are observed directly by polarized light microscopy. The results show that the driving force for crack propagation is the incompatible strain induced by 90° domain switching due to electric load only or the coupling of mechanical and electric loads. The sequence and path of the crack propagation are related to the initial domain structure and the characteristics of the external load.
© 2013 Acta Materialia Inc. Published by Elsevier Ltd. All rights reserved.

Keywords: Domain switching; Crack propagation; Coupling of mechanical and electric load; BaTiO$_3$ single crystal; Polarized light microscopy

Ferroelectrics have triggered much attention for their extensive applications, such as micro-electro-mechanical systems, actuators, transformers and sensors. However, one of the disadvantages is their brittleness, i.e. the internal cracks may nucleate and propagate after long-term working under external loads, resulting in the degradation of devices. The nucleation and propagation of the cracks is related to the domain configurations in ferroelectrics [1–3]. Recent studies have focused on a clear understanding of the crack growth and domain switching around the crack tips. Two examples of such studies are the modeling and the theoretical calculation of stress field around the crack tip [4–13], and the observation of domain switching and crack propagation under an external load [1,3,14–18]. However, the direct relationship between domain switching and crack propagation is not clear. Therefore, for more details, more studies by in situ observation are required, which can directly prove the theory of fracture behaviors in ferroelectrics. In our previous study, we looked at crack propagation and domain switching in a BaTiO$_3$ single crystal under external

fields [19,20]. It was found that the crack propagation is affected by the domain switching around the crack tip. Currently, there are very few direct observations about the correlation between domain switching and crack propagation under the coupling of mechanical and electric loads. In this study, domain switching and crack propagation in BaTiO$_3$ single crystals under mechanical and electric loads are investigated in situ by polarized light microscopy.

Two square BaTiO$_3$ single crystals with dimensions of 5 mm × 5 mm × 1 mm were used. Firstly, the upper (0 0 1) surfaces were polished carefully by diamond abrasive. Secondly, the samples were poled along the [0 1 0] direction. Thirdly, a penetrated notch of 0.3 mm wide and 1 mm long was prefabricated at the center of the 5 mm long edge, as depicted in Figure 1. A gradually increasing tensile load was then applied to the samples along the [1 0 0] direction using a homemade apparatus [21]. The loading was stopped when cracks appeared around the tips of the penetrated notches. After that, one sample (sample I) was removed from the loading apparatus and the other sample (sample II) remained. Thereafter, the electric field was applied to the samples along the [0 1 0] direction [22]. The selection of electric field intensity was based on the coercive field ($E_c = 250$ V mm^{-1}) of BaTiO$_3$ single crystal. The electric field

* Corresponding authors. Tel.: +86 10 13552349339; fax: +86 10 62332345; e-mail addresses: bingjiang@ncepu.edu.cn; baiy@mater.ustb.edu.cn
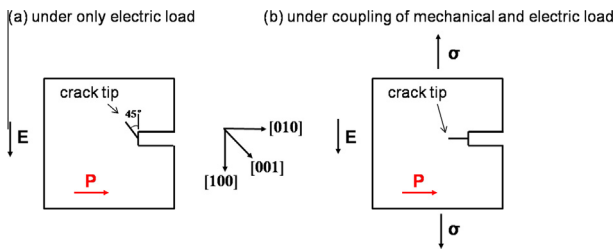
Figure 1. Schematic image of the samples under (a) electric load only and (b) coupling of mechanical and electric loads.

intensity was gradually increased until the cracks began propagating. The schematic diagrams of two samples under different external loading conditions are shown in Figure 1. The crack propagation and domain switching under the two loading conditions was in situ observed by an Olympus BX60 polarized light microscope (PLM).

The domains with polarization vectors along the $[100]$, $[\bar{1}00]$, $[010]$ and $[0\bar{1}0]$ directions are defined as a^+, a^-, b^+ and b^- domains, respectively. There are b^+ mono-domains on the (001) surface when the sample is polarized along the $[010]$ direction [22]. When a tensile load is applied along the $[100]$ direction, the domains switch to the $[100]$ or $[\bar{1}00]$ direction and become a^+ or a^- domains. In this work, many domain stripes appear in sample I after the tensile load is removed, as shown in Figure 2a. The result indicates that the system becomes a stable status with the 90° a–b domain structure. The polarization vectors of domain stripes are plotted as shown in the inset of Figure 2a, where the vectors of a^+ domains and b^+ domains connect head-to-tail and are perpendicular to each other. Meanwhile, a crack perpendicular to these domain stripes appears. When the electric field intensity is increased to a critical value, the crack begins to propagate. Figure 2 shows the crack propagation and domain switching around the crack in sample I under a critical electric field (E_1, 250 V mm^{-1}) only. For ease of observation, the bright spot **M** in Figure 2 is regarded as a reference point. With increasing time, the crack propagates gradually. With time, the a^+ domain stripes become

thicker and b^+ domain stripes become thinner, and this process complies with the domain switching criteria under an electric field [22]. After 1.5 h, the crack propagates from a to a_2, and a new crack **O** nucleates. The larger internal stress in this position leads to the nucleation and propagation of the new crack **O** and stops the propagation of the first crack. Although two cracks appear, their propagation characteristics are the same. It is considered that the whole crack propagation process is continuous. The evolution of the domain stripes is shown in the insets of Figure 2a, d, e and f. After 16 h, the crack stops propagating, as shown in Figure 2f, and all the observed areas become a^+ mono-domain, i.e. the polarization vectors of all domains are parallel to the direction of the external electric field.

Mechanical load can induce 90° domain switching and drive the polarization vector parallel to them. Since the mechanical load is applied in a line and does not refer to a certain direction and under sufficient load, the 180° multi-domain structure is formed instead of a^+ or a^- mono-domain. After the mechanical load is removed, the large depolarization energy of the 180° domain structure induces domain switching and a steady 90° multi-domain system is formed. The incompatible strain during 90° domain switching can result in crack propagation, which stops when the internal stress reaches equilibrium. Once an external electric field is applied to the sample, the equilibrium is broken by the electric-field-induced domain switching. The crack propagates due to the incompatible strain induced by 90° domain switching [16] and/or due to the electrostatic repulsion induced by the accumulated charges at cracks [23,24]. Since the crack is at an electrically permeable boundary condition in the BaTiO$_3$ single crystal, the first factor plays a dominant role in crack propagation. As can be seen in Figure 2, the domain switching on both sides of the crack is different because the crack cuts the domain stripes. From Figure 2e, it can be seen that domain stripes are only on one side of the crack. The incompatible strain induced by the 90° domain switching on both sides of the crack is the driving force for the crack propagation. Moreover, the crack always propagates along 45° and is perpendicular to
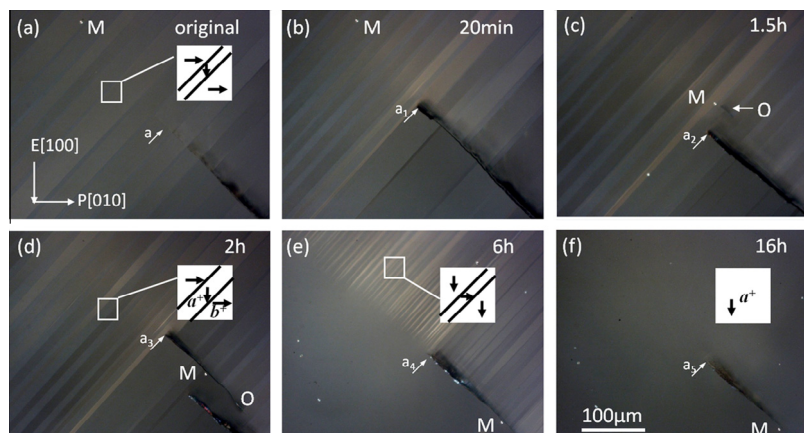
Figure 2. The domain switching and crack propagation of sample I with time under the sustained electric field ($E_1 = 250$ V mm^{-1}). The bright spot **M** in every panel is regarded as a reference point. The letters a–a_4, a_5 and the arrows show the crack propagation process. The insets depict the changes of the polarization vectors of a^+ and b^+ domains.
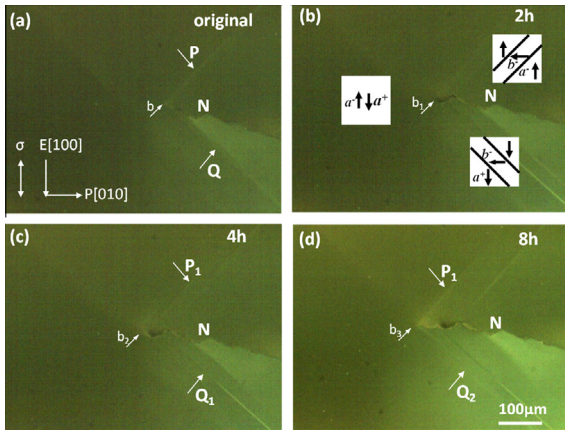
Figure 3. The domain switching and crack propagation of sample II with time under the coupling of electric and mechanical load ($E_2 = 100$ V mm^{-1}). The bend position **N** of the crack is regarded as the reference point. The letters **b–b$_3$** and the arrows show the crack propagation process. The letters **Q–Q$_2$**, **P–P$_1$** and the arrows show the changes of domain stripes around the crack tip. The insets show the 180° a–a domain structure at the front of the crack and 90° a–b domain structure around the crack tip, in which the letter and arrows refer to the polarization vectors of a^+, a^- and b^- domains.

Figure 4. The domain switching and crack propagation of sample II with time under the coupling of electric and mechanical load ($E_3 = 200$ V mm^{-1}). The bend position **N** of the crack is regarded as the reference point. The letters **c–c$_3$** and the arrows show the crack propagation process. The letters **A**, **A$_1$** and the arrows show the changes of domain stripes behind the crack tip. The inset show that the 180° a–a domain structure at the front of the crack.

the direction of domain stripes, which is the direction of internal shear stress [16].

Figures 3 and 4 show the crack propagation and domain switching around the crack tip of sample II under the coupling of mechanical and electric loads. When the electric load is applied to the sample II, no 90° domain switching is observed because of the sustained tensile load, as shown in Figure 3a. Therefore, the domains far away from the crack are 180° a^+ and a^- multi-domain structures, which cannot be distinguished by a PLM. Few domain stripes are observed at the crack tip, where the mechanical load is relaxed by the crack. Due to the sustained tensile load, the critical value of electric field intensity for crack propagation is found to be 100 V mm^{-1} (E_2), which is less than that under the electric load only (E_1, 250 V mm^{-1}). Figure 3 shows that the crack propagates from b to b_3, and the domain stripes around the crack tip keep their configurations (perpendicular to each other) and move with the crack propagation, as shown in Figure 3b–d. The bend position **N** of the crack in Figure 3 is regarded as a reference point. After 8 h, the crack and domain configuration does not change. Our previous studies showed that 180° domain switching consists of two 90° switching steps [22,25]. The 90° switching induces a shear force, resulting in crack propagation. As 90° domain stripes are always at a 45° angle to the load and the crack propagates perpendicular to the stripes, the crack is at 45° or 135° to the load [16]. When the crack propagates across one 180° domain and enters the adjacent one, the reverse polarization vector changes the direction of crack propagation by a 90° angle. The 90° domain switching always induces a shear force to open the crack and promote its propagation. As a result, the crack propagates in a zigzag manner.

When the electric field is increased to 200 V mm^{-1} (E_3), the crack tip propagates quickly in a straight manner, as shown in Figure 4. The bend position **N** of the

crack is also regarded as a reference point. Initially, the crack propagates from c to c_1, but the domain stripe A does not change, as shown in Figure 4a and b. Thereafter, a new domain stripe A1 appears at the crack tip c1, as shown in Figure 4c. Figure 4c and d depicts that the crack propagation occurs before changes of domain stripes. This result can be explained by 180° domain switching consisting of two 90° switching steps. Since 180° domain switching occurs at a very fast rate under coupling of mechanical load and a relatively high electric field, two 90° switching steps are too quick to be observed [22,25]. The driving force for crack propagation is the incompatible strain induced by two step 90° domain switching, although no domain stripes are observed in front of the crack.

From the observation above, domain switching and the crack propagation are different under different loading conditions, even though the incompatible strain induced by 90° domain switching is always the driving force for crack propagation. With the electric load only, the critical electric field intensity for crack propagation is high (E_1, 250 V mm^{-1}), and is equal to the critical field for domain switching, i.e. coercive field (E_c, 250 V mm^{-1}). Under the coupling of electric and mechanical loads, the critical electric field intensity for crack propagation is low (E_2, $E_3 < E_c$). It is our considered view that the critical field for crack propagation can be decreased by the coupling of mechanical load and electric field.

In summary, the behaviors of crack propagation and domain switching under different loading conditions were in situ investigated by polarized light microscopy. The results show that the driving force for crack propagation is always the incompatible strain induced by 90° domain switching. The sequence and path of crack propagation are attributed to the initial domain structure and the characteristics of external loads. Under an electric load only, the crack propagation needs a high electric field equal to coercive field and it is perpendicular to the 90° domain stripes. Application of a mechanical load

in same direction lowers the critical electric field for crack propagation. In this case, the crack propagation is induced by the two step 90° switching in 180° domain switching. When the electric field is relatively low, the crack propagates in a zigzag manner. When the electric field is high, the crack propagates at a fast rate and in a straight manner. The observed phenomena in this work are useful in understanding the correlations between fracture behavior and the domain switching process.

[1] F. Wang, Y.J. Su, J.Y. He, L.J. Qiao, W.Y. Chu, Scripta Mater. 54 (2006) 201–205.
[2] R.M. Wang, W.Y. Chu, Y.J. Su, J.X. Li, L.J. Qiao, Mater. Sci. Eng. B 135 (2006) 141–144.
[3] D. Fang, Y. Jiang, S. Li, C.T. Sun, Acta Mater. 55 (2007) 5758–5767.
[4] A. Abdollahi, I. Arias, Acta Mater. 59 (2011) 4733–4746.
[5] A. Abdollahi, I. Arias, J. Mech. Phys. Solids 60 (2012) 2100–2126.
[6] H. Qiao, J. Wang, W. Chen, Acta Mech. Solida Sin. 25 (2012) 1–8.
[7] D.K. Aaadzierski, E.V. Kirichenko, V.A. Stephanovich, Phys. Lett. A 375 (2011) 685–688.
[8] W. Li, C.M. Landis, Eng. Fract. Mech. 78 (2011) 1505–1513.
[9] M. Kuna, Eng. Fract. Mech. 77 (2010) 309–326.
[10] T.Y. Zhang, C.F. Gao, Theoret. Appl. Fract. Mech. 41 (2004) 339–379.
[11] Y. Zhang, J. Li, D. Fang, J. Mech. Phys. Solids 61 (2013) 114–130.
[12] G.Z. Mao, D.N. Fang, Theoret. Appl. Fract. Mech. 41 (2004) 115–123.
[13] P. Neumeister, H. Kessler, H. Balke, Acta Mater. 58 (2010) 2577–2584.
[14] Y. Jiang, D. Fang, Scripta Mater. 57 (2007) 735–738.
[15] C. Leach, N.K. Ali, D.A. Hall, Ceram. Int. 37 (2011) 2185–2191.
[16] Y.W. Li, F.X. Li, Scripta Mater. 67 (2012) 601–604.
[17] Y. Jiang, D. Fang, Mater. Lett. 61 (2007) 5047–5049.
[18] X. Tan, Z. Xu, J.K. Shang, P. Han, Appl. Phys. Lett. 77 (2000) 1529–1531.
[19] B. Jiang, Y. Bai, J.-L. Cao, Y. Su, S.-Q. Shi, W. Chu, L. Qiao, J. Appl. Phys. 103 (2008) 116102.
[20] B. Jiang, X. Xing, Z. Guo, Acta Metall. Sin. 47 (2011) 605–610.
[21] L. Shen, J. He, Y. Su, W. Chu, L. Qiao, Acta Metall. Sin. 42 (2006) 810–814.
[22] B. Jiang, Y. Bai, W. Chu, Y. Su, L. Qiao, Appl. Phys. Lett. 93 (2008) 152905.
[23] X. Sun, Y.J. Su, K.W. Gao, L.Q. Guo, L.J. Qiao, Scripta Mater. 66 (2012) 292–295.
[24] X. Sun, Y.J. Su, K.W. Gao, L.Q. Guo, L.J. Qiao, W.Y. Chu, T.-Y. Zhang, J. Am. Ceram. Soc. 94 (2011) 4299–4304.
[25] P.L. Liu, W.Y. Chu, L.J. Qiao, Int. J. Miner. Metall. Mater. 17 (2010) 494–499.